

## Correlation of Measured Fractal Dimensions with Lacunarities in Computer-Generated Three-Dimensional Images of Cantor Sets and Those of Fractional Brownian Motion

Masaharu DOMON and Eiichi HONDA

*Department of Dental Radiology and Radiation Research, Tokyo Medical and Dental University,  
1-5-45 Yushima, Bunkyo-ku, Tokyo 113-8549, Japan*

(Received August 5, 1999; Accepted October 25, 1999)

**Abstract.** Three-dimensional images constructed by CT and MRI has been recently taken as routine diagnosis in medicine and so measures such as fractal dimensions. Lacunarities for 3-dimensional networks or textures are expected to be used as diagnostic parameters. The method of moments and the box counting method to estimate the fractal dimensions of images were examined for their reliability, using images with theoretical fractal-dimensions, which computationally implemented from 3-dimensional triadic Cantor sets and 3-dimensional fractional Brownian motion. In addition, correlation between the deviations of the measured dimensions from the theoretical ones and lacunarities was analyzed. The lacunarity,  $A$ -dila was defined using a morphological filter of 3-dimensional dilation of an image. It was found that the measured fractal-dimensions by the method of moments were well fit to the theoretical ones for those images with less  $A$ -dila's, however, significantly deviated for those images with larger  $A$ -dila's. Thus, the method of moments is expected to estimate sufficiently accurate fractal dimensions of textures in 3-dimensional medical images with less  $A$ -dila's.

### 1. Introduction

The fractal dimensions of medical 2-dimensional images are accepted as useful evaluations of branching structures or networks of tissues in diagnosing diseases (BYNG *et al.*, 1997; HONDA *et al.*, 1992; PEISS *et al.*, 1996; THIELE *et al.*, 1996; VEENLAND *et al.*, 1996). The digitizing technology has these days greatly progressed to allow construction of 3-dimensional images in biology (STREICHER *et al.*, 1997), and to numerically analyze 3-dimensional medical images constructed by CT and MRI (LAINE *et al.*, 1997; SERNETZ *et al.*, 1992) with a satisfactory speed of computation. Therefore, the present study has primarily attempted to assess methods to measure fractal dimensions of the 3-dimensional medical images in order to apply the dimensions as supplementary parameters in diagnosing diseases such as osteoporosis (CHUNG *et al.*, 1994; HAIDEKKER *et al.*, 1997; MAJUMDAR *et al.*, 1997).

Such assessment needs to take account of some problems on the nature of fractal dimensions. Firstly, the measured fractal dimension of an image is not unique yielding different values depending on the range of measuring scales (VOSS, 1988; EVERTSZ and

MANDELBROT, 1992). Secondly, fractal sets with the same fractal dimension give rise to images with different textures depending on the lacunarities as discussed by MANDELBROT (1983, 1994). For example, a triadic 1-dimensional Cantor set on the full closed interval of  $[0,1]$  with segmentation factor of  $1/r = 3$  and  $N = 2$  segments to leave has the same Hausdorff-Bescovitch dimension,  $D = (\log 2)/(\log 3)$  as any sets with  $1/r = 3^k$  and  $N = 2^k$  for integer  $k(k > 1)$ . However, the texture and the dimension measured by a box counting method are quite different with increased  $N(k \gg 1)$  depending on the arrangement of distribution of  $N$  segments on the interval  $[0,1]$ ; the measured dimension,  $\text{Dim} \approx 0$  when the  $N$  segments are densely-shifted to near ends of the interval  $[0,1]$  with a large gap in its center, while  $\text{Dim} \approx 1$  when they are uniformly-spaced in the interval. Thirdly, digitized images of fractal sets due to their discretized nature do not conform to the mathematics of fractal geometry, by which fractal dimension is defined by the power law in a range of infinitesimally-decreased scales of  $\varepsilon$ , or by Minkowski sausage (MANDELBROT, 1983).

Previous studies on 2-dimensional images by others showed large discrepancies (0.2 to 0.3) between their measured fractal-dimensions and theoretical ones (KELLER *et al.*, 1989; HUANG *et al.*, 1994), which led to a view that absolute values of fractal dimensions could not be measured and only the relative values were reliable. These images were those of 2-dimensional fractional Brownian motion, which treated as the surfaces in 3-dimensional space (Brownian surfaces). That is, the Brownian values  $f(x,y)$  were taken on  $z$ -axis. KELLER *et al.* (1989), recognized that points on the surface were widely spaced and so these contributed to lower the values of measured fractal-dimensions. To solve this problem we have taken an algorithm to generate 2-dimensional binary images of the Brownian surfaces by the mean values of points, i.e.  $f(x,y) = 1$  if  $|z - \text{mean}| \leq \varepsilon$ , else  $f(x,y) = 0$ . These binary images gave accurate estimates of the fractal dimensions and correlation between the fractal dimensions and lacunarities was observed (DOMON *et al.*, 1998).

The present study attempts to extend the 2-dimensional algorithms to 3-dimensional ones and to investigate whether 3-dimensional binary images implemented can be used as standard fractal-images and the methods to measure the fractal dimensions and lacunarities are reliable.

## 2. Methods

### 2.1. Implementation of 3-dimensional fractal images

#### 2.1.1. 3-dimensional triadic Cantor sets

Images were generated by the iteration; the initiator is a filled unit-cube and the generator is to cut it into 27 ( $= 3 \times 3 \times 3$ ) segments of cubes ( $r = 1/3$ ), among which  $N$  segments are left for the next cut. Therefore, after  $k$  iterations the number of segments left increases as  $N^k$  from  $27^k$  of total number of segments. The Hausdorff-Bescovitch dimension,  $D$  is related to  $N$  by  $D = (\log N)/(\log 3)$ . Figure 1 illustrates representative generators of 3-dimensional triadic Cantor sets as follows. The cross-sections of  $xy$ -planes of 27 segment-cubes of the generator were grouped as 3 layers of Bottom, Middle and Top with 9 segment-cubes per layer. The segment-cubes were named as #0 to #26 by the rule; those of the bottom row of Bottom layer were numbered as #0, #1, #2 from the left, those of the middle row as #3, #4, #5 and those of the top row as #6, #7, #8. The segments of Middle and Top layer were named by the similar sequences. For example, the generator of a  $N = 3$  set shown

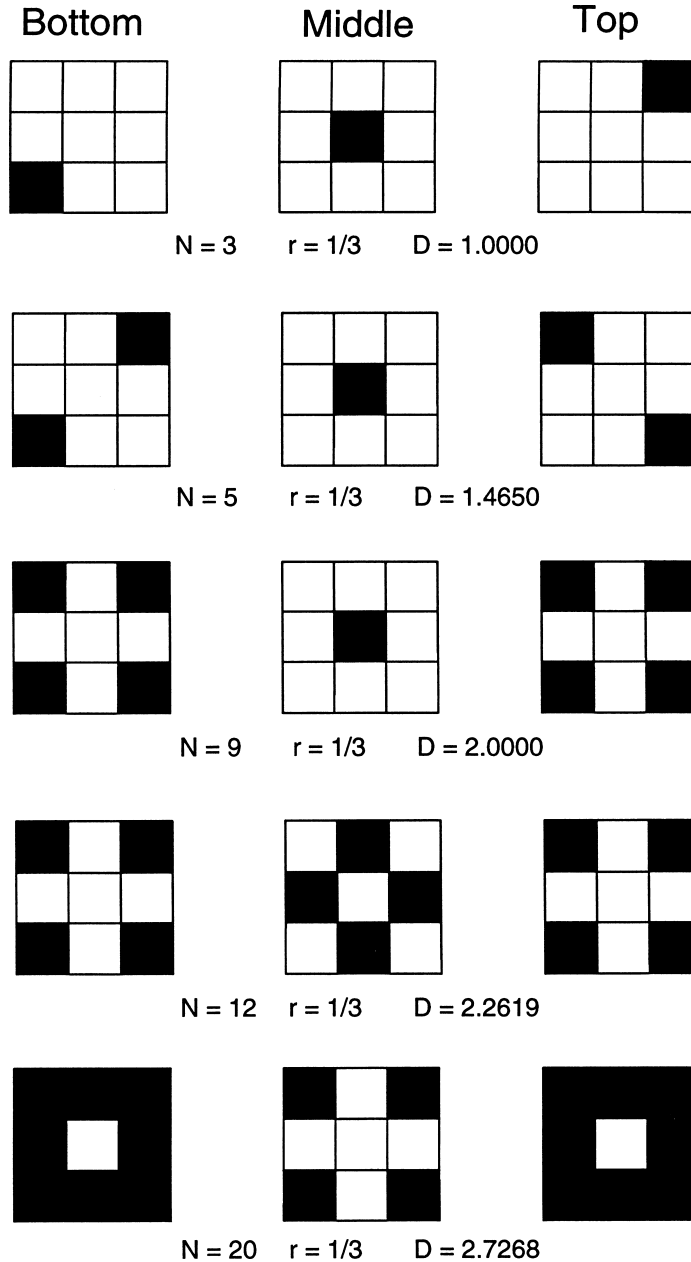


Fig. 1. Representative generators of 3-dimensional triadic Cantor sets with an initiator of filled box. At each iteration step, a cube is cut into 27 segment-cubes grouped as Bottom (#0–#8 segment), Middle (#9–#17 segment) and Top layer (#18–#26 segment), of which  $N$  segments are left for the next iteration. The segments in Bottom layer are sequentially numbered as #0 to #3 from left to right for the bottom row, #3 to #5 for the middle row and #6 to #8 for the top row and those of other layers are numbered in a similar way.

in Fig. 1 was to leave #0, #13 and #26 segment-cube as indicated by closed squares. Twenty images of the Cantor sets were implemented in this study; 3 images with  $N = 3$ , 4 images with  $N = 5$ , 6 images with  $N = 9$ , 3 images with  $N = 12$  and 4 images with  $N = 20$ . The image called as a Menger sponge shown in Fig. 2 is visualized by volume rendering of a  $N = 20$  set, of which generator is seen in Fig. 1 (MANDELBROT, 1983).

The array size of all images was fixed at  $244 \times 244 \times 244$  with addresses of  $x, y, z$  from 0 to 243, and the generator was operated by 5 iterations. Thus, the size of a final segment-cube left became  $1 \times 1 \times 1$  with addresses of 8 vertices. After initialization of  $244 \times 244 \times 244$  array with setting to 0, the binary image was constructed from the image array for the final segment-cubes by giving 1 to only one vertex and 0 to the other 7 vertices for any final segment-cube. Figure 3 presents an image of the  $N = 9$  set which displayed as three 2-dimensional binary images of  $xy$ -planes at  $z = 0, 1$  and 2 (its generator is seen in Fig. 1).

### 2.1.2. Sets of 3-dimensional fractional Brownian motion

Three-dimensional sets of fractional Brownian motion is defined by

$$\text{Variance}\{f(\mathbf{R}_i) - f(\mathbf{R}_j)\} \propto |\mathbf{R}_i - \mathbf{R}_j|^{2H}, \quad 0 < H < 1$$

where  $\mathbf{R}_i, \mathbf{R}_j$  are points in 3-dimensional space. Images of the sets for given  $H$  were implemented by a method modulated from an algorithm named as midpoint displacement and successive random additions for 2-dimensional fractional Brownian motion (SAUPE, 1988). The image size was  $129 \times 129 \times 129$ . The method constructed 3-dimensional arrays of  $f(x, y, z) = \text{value}$ , which were then converted to 3-dimensional binary data by the mean

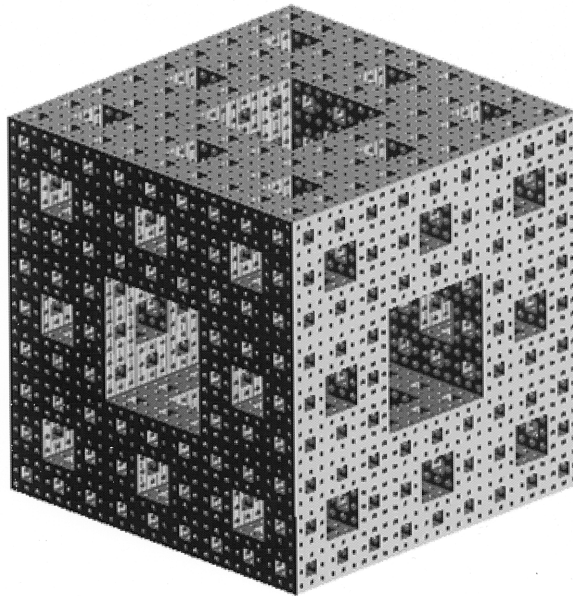


Fig. 2. A visualized image of a 3-dimensional triadic Cantor set with  $N = 20$  (a Menger sponge), of which generator is shown in Fig. 1.

of values;  $f(x, y, z) = 1$  if  $|f(x, y, z) - \text{mean}| \leq \varepsilon$ , else  $f(x, y, z) = 0$ . The value of  $\varepsilon$  was set to 0.125, when the standard deviation of the nearest point-to-point distribution was fixed at 0.5 for any image. By this conversion, the fractal dimension,  $D$  was related to  $H$  by  $D \approx 3 - H$  (VOSS, 1988). Ten 3-dimensional images per  $H$  ( $H = 0.3$  to 0.9 with a step of 0.1) were generated and so total number of images generated was 70. Figure 4 presents the image of a  $H = 0.3$  set (theoretical fractal dimension of 2.7) visualized by volume rendering after operation of 3-dimensional morphological filter of closing by structuring element of  $3 \times 3 \times 3$  (SERRA, 1992).

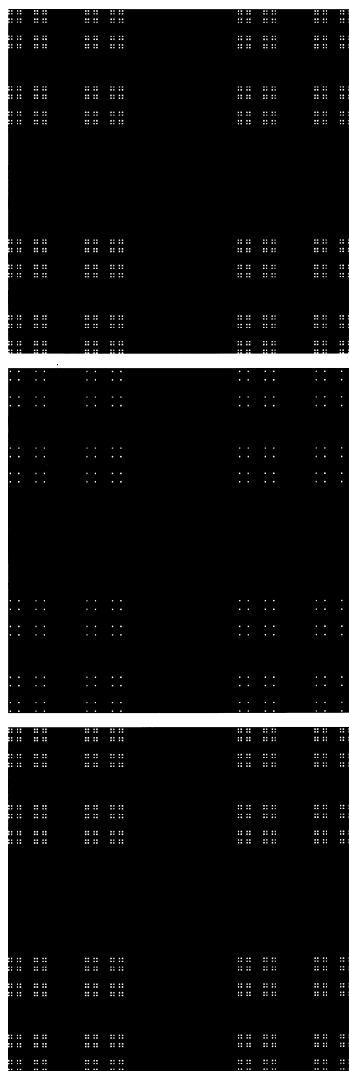


Fig. 3. Two-dimensional displays at  $z = 0$ ,  $z = 1$  and  $z = 2$  of a 3-dimensional triadic Cantor set with  $N = 9$ , of which generator is shown in Fig. 1.

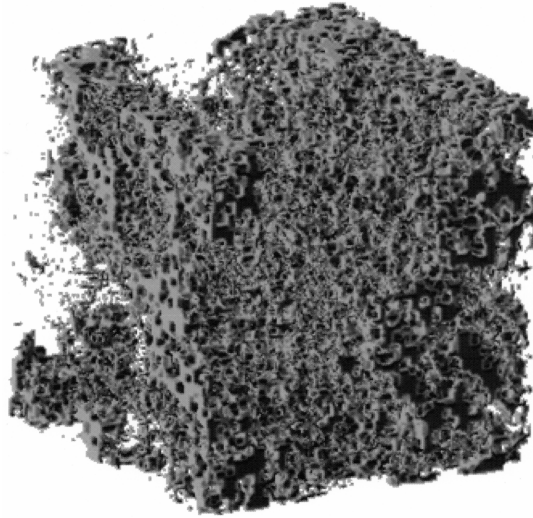


Fig. 4. A visualized image of fractional Brownian motion with  $H = 0.3$  (theoretical fractal dimension = 2.7) operated by closing of a 3-dimensional morphological filter.

## 2.2. Methods of fractal-dimension measurement

The method of moments was based on the following algorithm (VOSS, 1988). When  $P(m, L)$  is the probability that a cube of size  $L$  centered on any point of a binary image covers  $m$  points ( $\sum P(m, L) = 1$ ) and so  $mP(m, L)$  is the moment, the mass  $M(L) = \sum mP(m, L)$  is related to the fractal dimension  $D$  by  $M(L) \propto L^D$ . The measuring scale,  $L$  was spanned from 3 to 31 by 15 steps with a step size of 2.

An alternative method to measure the fractal dimension, a box counting method (HUANG *et al.*, 1994) was investigated. The measuring scales,  $L$  was spanned as powers of 2, that is, from 4 to 64 for images of the Cantor sets and from 4 to 32 for images of the fractional Brownian motion.

## 2.3. Lacunarity measurement

The various measures of lacunarity,  $\Lambda$  are defined by MANDELBROT (1983, 1994), VOSS (1988) and KELLER *et al.*, (1989). In the present study, the two measures were investigated.

### 2.3.1. Lacunarity defined by 3-dimensional dilation

The measure of lacunarity was defined by Minkowski sausage for a 1-dimensional Cantor set (MANDELBROT, 1994). In the present study it was modulated to the one for a 3-dimensional binary image with using a 3-dimensional morphological filter of dilation (SERRA, 1992). That is, the lacunarity was defined as  $\Lambda\text{-dila} = n\text{-dila} / (n \times 27)$ , where  $n$  is the number of points of an original 3-dimensional binary image and  $n\text{-dila}$ , the number of points of image dilated by  $3 \times 3 \times 3$  structuring element. Since  $n\text{-dila}$  is equal to  $n \times 27$  by operation of 3-dimensional dilation filter on an image, of which points are separated from any other points with a distance of more than 2 digitized addresses in any direction of

$x$ -,  $y$ -, and  $z$ -axis, its lacunarity is 1.0. By the dilation operation on a digitized image of Euclidean solid objects ( $E = 3$ ), its dilated image remains as the original one and so the lacunarity is  $1/27$ . A digitized image of the straight line ( $E = 1$ ) yields  $\Lambda\text{-dila} = 9/27$  and that of the plane ( $E = 2$ ),  $\Lambda\text{-dila} = 3/27$ . Thus,  $1/27 \leq \Lambda\text{-dila} \leq 1$ .

### 2.3.2. Lacunarity defined by moments

When  $P(m, L)$  is probability that the box with size  $L$  centered on a point contains  $m$  points,  $q$ -th moment of  $P(m, L)$   $M^q(L) = \sum m^q P(m, L)$ . As mentioned before  $M(L)$  is the mass of  $P(m, L)$ . The measure of lacunarity proposed by VOSS (1988) is defined as  $\Lambda\text{-moment} = \{M^2(L) - M(L)^2\} / M(L)^2$ . When points are uniformly distributed in the range of measuring box size,  $m \cong \text{constant}$  and so  $\Lambda\text{-moment} \cong 0$ . Therefore, an image in which points are isolated ( $m = 1$ ) or compactly -filled in measuring box gives  $\Lambda\text{-moment} \cong 0$ .

## 3. Results

### 3.1. Measured fractal dimensions of triadic Cantor images

The mass  $M(L)$  of a 3-dimensional binary image was in general fit to a straight line of  $\log M(L) - \log L$  plot as expected. The fractal dimensions of triadic Cantor images calculated from  $\log M(L) - \log L$  plot (method of moments) were compared with the theoretical ones (Fig. 5). The line in the figure indicates a complete fit between the measured fractal-dimensions and theoretical ones. However, when the deviation is supposed as  $\Delta = |\text{measured fractal dimension} - \text{theoretical fractal dimension}|$ , the  $\Delta$ 's larger than

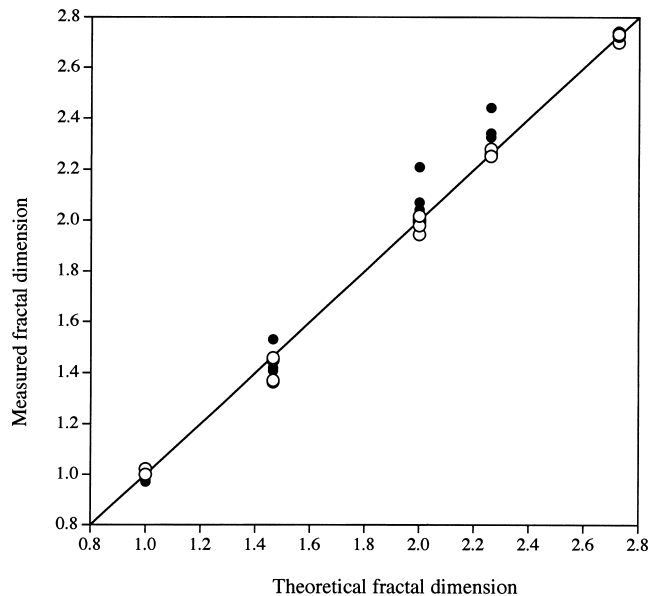


Fig. 5. The measured fractal dimensions of images of the Cantor sets plotted as a function of theoretical fractal dimension. The open circle indicates the data by the method of moments and the closed circle, by the box counting method.

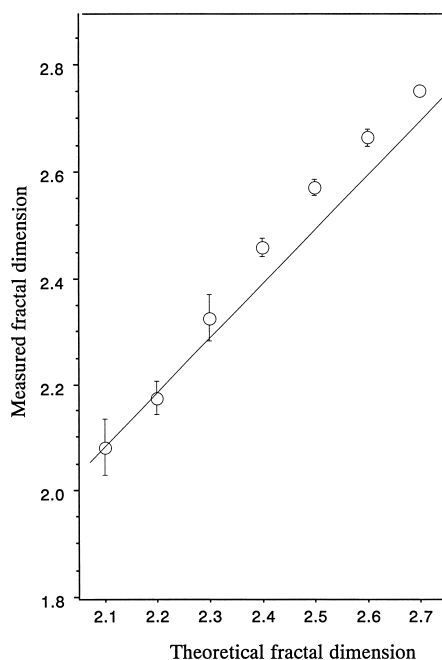
0.02 were investigated in 6 out of 20 images. The largest  $\Delta > 0.1$  was given by the data for a  $N = 5$  image, of which theoretical fractal dimension is 1.4650.

The box counting method gave exactly the same value of fractal dimension as the theoretical one for any image of the Cantor sets when measuring scale  $L$ 's were chosen as power of 3. Such complete fit was reasonable since images of the triadic sets were implemented by the generators with  $r = 1/3$  (see, Fig. 1). Therefore such measurements are only significant in confirming the error-free of the program to implement images of the Cantor sets and so not concerned in further analyses. As mentioned in Sec. 2, the data by box counting method was obtained by the measuring scales of power 2.

The data by the box counting method are superimposed in Fig. 5 (closed circles). It is evident that the deviation  $\Delta$ 's are in general larger than those by the method of moments. In fact, the deviation  $\Delta$ 's are larger than 0.02 in 15 cases out of 20 Cantor sets investigated. The largest deviation  $\Delta = 0.21$  was seen for a  $N = 9$  image with theoretical fractal-dimension of 2.0.

### 3.2. Measured fractal-dimensions of images of fractional Brownian motion

The data by the method of moments and box counting method are plotted in Figs. 6a



(a)

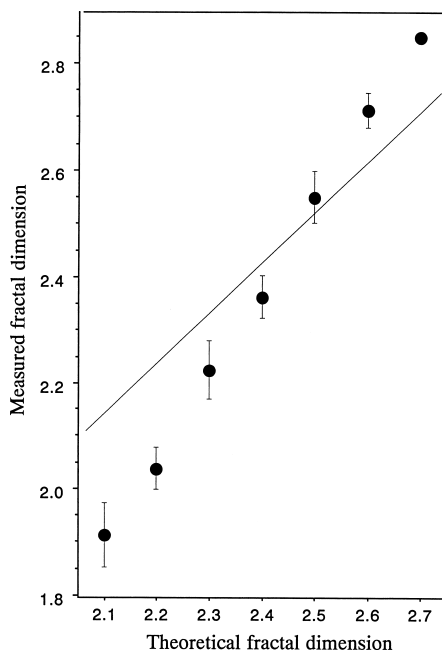
Fig. 6. The measured fractal dimensions of images of the fractional Brownian motion plotted as a function of theoretical fractal dimension. The open circle indicates the data by the method of moments (Fig. 6a) and the closed circle, by the box counting method (Fig. 6b). Each point and bar indicates means and standard error, respectively.

and 6b, where the points indicate the averaged values of 10 images with given  $H$ 's. The straight line is drawn as a complete fit between the measured fractal-dimensions and the theoretical ones. The averaged dimensions by the method of moments (open circles in Fig. 6a) were deviated from the theoretical ones with  $\Delta < 0.07$ , and the  $\Delta$ 's by the box counting method were larger (closed circles in Fig. 6b).

### 3.3. Lacunarities measured by the dilation method

The lacunarities measured by the dilation method,  $\Lambda$ -dila for images of the Cantor sets are shown in Fig. 7 as a function of fractal dimension measured by both the methods (open circles for the method of moments and closed ones, for the box counting method). The points marked by star indicate Cantor sets with the deviation  $\Delta > 0.05$ , and those marked by double stars or by "star +" indicates the set of  $\Delta > 0.18$  or  $\Delta > 0.2$ , respectively. It appears that the  $\Delta$  for the measured fractal-dimension by the method of moments is correlated with the  $\Lambda$ -dila; the larger  $\Lambda$ -dila, the larger  $\Delta$ . This is not the case for the box counting method.

The images of sets, of which points are rather widely spaced, yielded the largest lacunarities among images of sets with the same  $N$  of 5, 9, 12, and 20, respectively. The image of  $N=5$  set (theoretical fractal-dimension = 1.4650) yielded lacunarity of 0.7126 and



(b)

Fig. 6. (continued).

the dimension deviation  $\Delta = 0.1$  (its generator is seen in Fig. 1). The image of  $N = 9$  set (theoretical fractal-dimension = 2.0) yielded lacunarity of 0.4895 (its 2-dimensional displays in Fig. 3). In contrast, the lacunarity of 0.1577 was given by the image of a  $N = 9$  set, of which points are densely arranged. Its generator is of combination of #0#1#3/#9#10#12/#18#19#20 segment (the rule described in Sec. 2) and the 3-dimensional image is composed of thin rods with  $L$ -formed cross-sections (image not shown). When the dimension measurement was carried out on this image by the box counting method,  $\Delta = 0.21$  (data point marked by “ $\star+$ ” in Fig. 7).

The lacunarities,  $\Lambda$ -dila's of images of 3-dimensional fractional Brownian motion are shown in Fig. 8a or in Fig. 8b as a function of fractal dimension measured by the method of moments or by the box counting method, respectively. In both the figures the data of three sets with theoretical dimensions of 2.1, 2.4 and 2.6 ( $H = 0.9, 0.6,$  and  $0.4,$  respectively) are plotted, where a cluster of 10 points corresponds to data of a group with a given  $H$ . The  $\Lambda$ -dila's were decreased with increased fractal-dimensions in a way similar to those of the Cantor sets. In addition these figures indicate that the measured fractal-dimensions are widely scattered for the images with 2.1 of theoretical fractal-dimension and that the extents of data scattering are larger for the data by the box counting method.

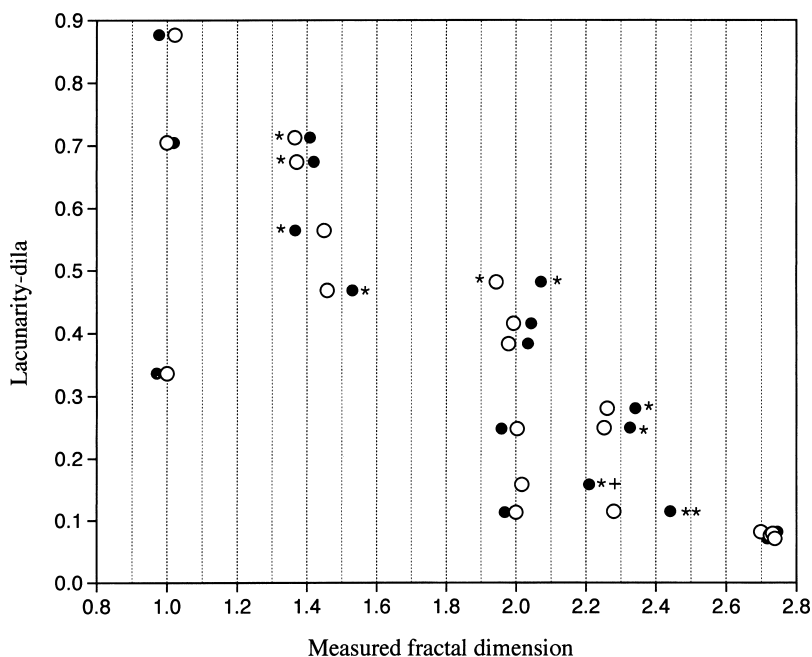
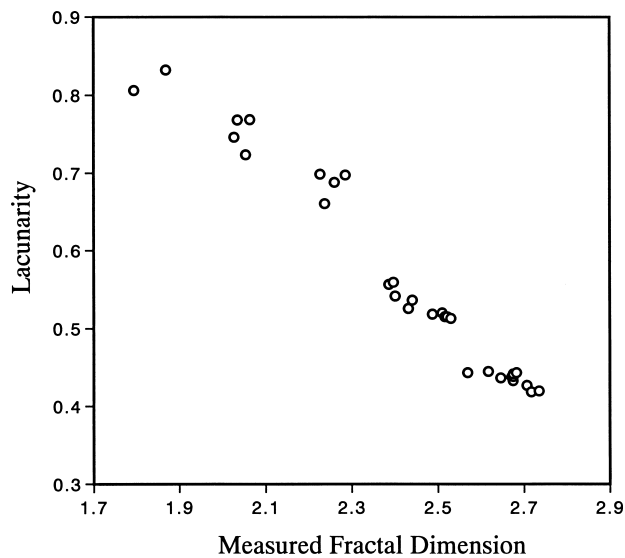
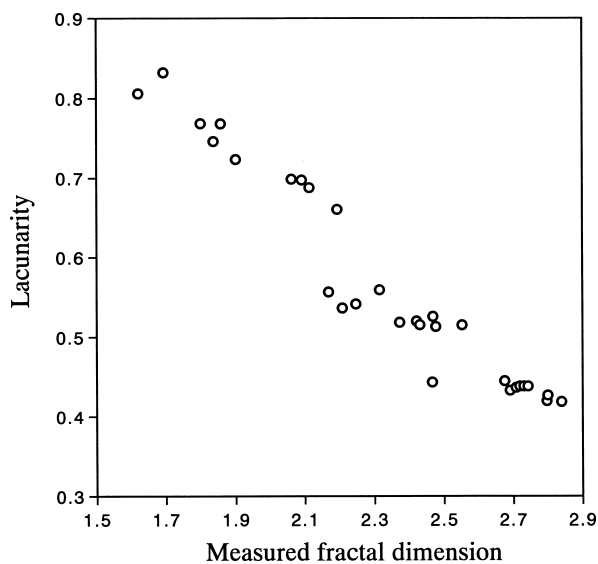


Fig. 7. Correlation of the lacunarity-dila's with the theoretical fractal dimensions of images of the Cantor sets. The open circle indicates the data by the method of moments and the closed circle, by the box counting method. The points marked by  $\star$ ,  $\star\star$  or  $\star+$  indicate the data of the images with  $\Delta > 0.05$ ,  $\Delta = 0.18$  or  $\Delta = 0.21$ , respectively. The  $\Delta$  is defined in the text.



(a)



(b)

Fig. 8. The lacunarity-dila's of the images of fractional Brownian motion plotted as a function of the fractal dimension measured by the method of moments (Fig. 8a) and by the box counting method (Fig. 8b). The data of three groups are plotted. The group is composed of 10 images with  $H = 0.9$  (theoretical fractal dimension = 2.1),  $H = 0.6$  and  $H = 0.4$ , respectively.

### 3.4. Lacunarities measured by the moment method

The lacunarities,  $\Lambda$ -moment's of the Cantor set images are plotted in Fig. 9. The correlation between the  $\Lambda$ -moments and the measured fractal-dimensions cannot be found. In Fig. 10 both the lacunarities, the  $\Lambda$ -dila's and  $\Lambda$ -moment's are compared for the fractional Brownian motion images. It can be seen that the  $\Lambda$ -moment's are more widely scattered within 10 images of a  $H$  and shows no tendency in their changes with increased theoretical fractal-dimensions. Similar results were obtained by using the scaling size  $L = 5$  for the measurements of lacunarities of images by both the methods.

## 4. Discussion

### 4.1. 3-dimensional images as standards for fractal dimension measurements

The implemented images of fractal sets are not true fractals due to their discretization and limited resolution (KELLER *et al.*, 1989; AVNIR *et al.*, 1998). A question may be raised whether or not 3-dimensional images in this study can be applied as the standards for assessing a method to measure fractal-dimensions. As described in Sec. 3 most images of the Cantor sets are confirmed to provide measured fractal-dimensions fit to their theoretical ones and so at least, those images with lower  $\Lambda$ -dila lacunarities are expected to be candidates for such standard images.

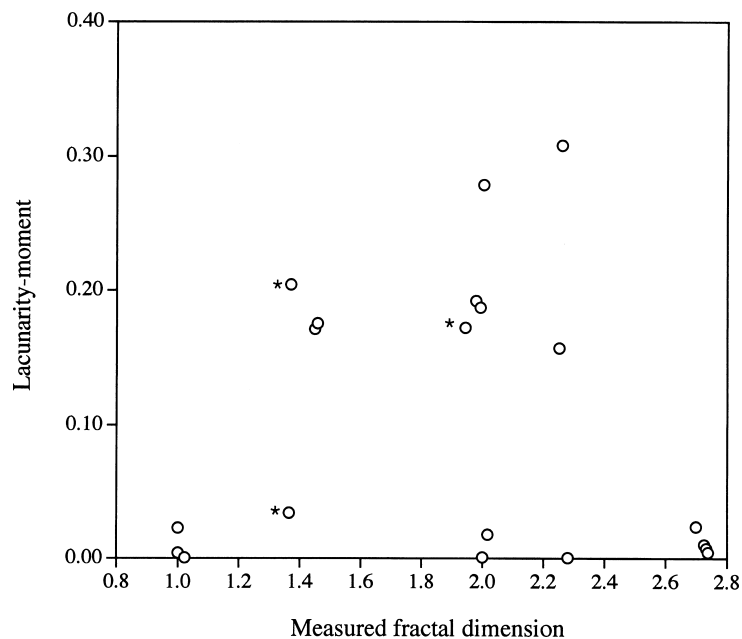


Fig. 9. The lacunarity-moment of images of the Cantor sets plotted as a function of the fractal dimension measured by the method of moments. The points marked by  $\star$  indicates the data with  $\Delta > 0.05$ .

Since textures in medical images are, in general, of irregular pattern unlike the Cantor sets, the images of fractional Brownian motion may be useful as the standards. It remains a question whether these images implemented by the algorithm in the present study are reliable as the standards. We have attacked the question by the 1-, 2- and 3-dimensional images of fractional Brownian motion with scanning  $H$ 's, variances of values between nearest neighbors and the binary widths,  $\varepsilon$ 's (see, Sec. 2). The settings described in Sec. 2 are found to be satisfactory to give the measured fractal dimensions closer to theoretical ones for images with  $H = 0.9$  to  $0.3$ . However, the images of sets with less  $H$ 's were more similar to those images of white noise and so the images with  $H < 0.2$  were not described. Even those images with  $H \geq 0.3$  are widely scattered in their measured dimensions and lacunarities, which reflects a statistical nature in the point-distributions of images. Thus, the images of fractional Brownian motion with  $H = 0.3$  to  $0.9$  can be used as the standards for fractal analysis, when the collected data from 10 or more images with a single  $H$  are assayed.

#### 4.2. Methods to measure fractal dimensions of images

Small deviations were not observed in measurement of fractal dimensions of fractional Brownian motion images (Figs. 8a and 8b). The deviations may result from a method. However, the method of moments has been assessed to be reliable in the measurements of

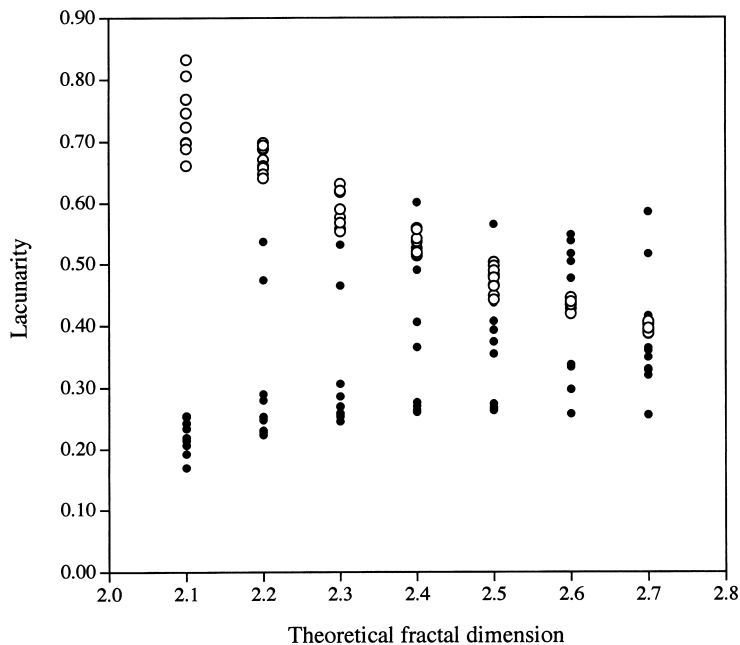


Fig. 10. The values are compared in the images of fractional Brownian motion between the lacunarity defined by the dilation method,  $\Lambda$ -dila (open circles) and that defined by the moment method,  $\Lambda$ -moment (closed circles).

the fractal dimension of an 3-dimensional image except for cases with larger lacunarities,  $\Lambda$ -dila. In contrast, the box counting method, in general, provides rather larger deviations, the  $\Delta$ 's. The reason for this was given by EVERTSZ and MANDELBROT (1992) as follows. The box counting method counts the number of boxes of size,  $L$  to cover an image when the box contains a single point, a few points or even large number of points, respectively. In other words the number of boxes  $N(L)$  is counted without taking into consideration of the weights of points.

#### 4.3. Lacunarity and noise

The results lead to the conclusion that the measure of lacunarity defined by the dilation,  $\Lambda$ -dila of an image is preferable to the one by the moment method and gives the correlation between lacunarities and fractal dimensions. In addition the present study indicates the influence of noise which is universal in medical images. When the noise level is high, the moment  $mP(m, L)$  is increased resulting in the larger fractal dimension. Inversely, the noise at a lower level is added to images with lower theoretical fractal-dimensions, the isolated points are widely positioned and so the moment  $P(1, L)$  becomes significant resulting in lowering the measured fractal-dimensions and increasing the  $\Lambda$ -dila's. Thus, it may be essential to remove the noise of images prior to the measurements of their fractal dimensions.

The work has been partly supported by Grant-in-Aid of Japanese Ministry of Education, Culture and Sports, Grant # 08672150.

#### REFERENCES

- AVNIR, D., BIHAM, O., LIDAR, D. and MALCAI, O. (1998) Is the geometry of nature fractal?, *Science*, **279**, 39–40.
- BYNG, J. W., YAFFE, M. J., LOCKWOOD, G. A., LITTLE, L. E., TRITCHLER, D. L. and BOYD, N. F. (1997) Automated analysis of mammographic densities and breast carcinoma risk, *Cancer*, **80**, 66–74.
- CHUNG, H.-W., CHU, C.-C., UNDERWEISER, M. and WEHRLI, F. W. (1994) On the fractal nature of trabecular structure, *Med. Phys.*, **21**, 1535–1540.
- DOMON, M., HONDA, E. and SASAKI, T. (1998) Two dimensional images of fractal sets and their usefulness in analysis of the method of dimension measurement, in *CAR'98—Computer Assisted Radiology and Surgery* (ed. H. U. Lemke, M. W. Vannier, K. Inamura and A. G. Farman), Elsevier, Amsterdam, p. 972.
- EVERTSZ, C. J. G. and MANDELBROT, B. B. (1992) Multifractal measures in *Chaos and Fractals New Frontiers of Science* (ed. H.-O. Peitgen, H. Jürgens and D. Saupe), Springer-Verlag, New York, pp. 922–953.
- HAIDEKKER, M. A., ANDRESEN, R., EVERTSZ, C. J. G., BANZER, D. and PEITGEN, H.-O. (1997) Assessing the degree of osteoporosis in the axial skeleton using the dependence of the fractal dimension on the grey level threshold, *Brit. J. Radiol.*, **70**, 586–593.
- HONDA, E., DOMON, M., SASAKI, T., OBAYASHI, N. and IDA, M. (1992) Fractal dimensions of ductal patterns in the parotid glands of normal subjects and patients with Sjögren syndrome, *Invest. Radiol.*, **27**, 790–795.
- HUANG, Q., LORCH, J. R. and DUBES, R. C. (1994) Can the fractal dimension of images be measured?, *Pattern Recognition*, **27**, 339–349.
- KELLER, J. M., CHEN, S. and CROWNOVER, R. M. (1989) Texture description and segmentation through fractal geometry, *Comput. Vis. Graph. Image Proc.*, **45**, 150–166.
- LAINE, H.-J., KONTOLA, K., LEHTO, M. U. K., PITKÄNEN, M., JARSKE, P. and LINDHOLM, T. S. (1997) Image processing for femoral endosteal anatomy detection: description and testing of a computed tomography based on program, *Phys. Med. Biol.*, **42**, 673–689.
- MAJUMDAR, S., GENANT, H. K., GRAMPP, S., NEWITT, D. C., TRUONG, V. H., LIN, J. C. and MATHUR, A. (1997)

- Correlation of trabecular bone structure with age, bone mineral density and osteoporotic status- in vitro studies in the distal radius using high resolution magnetic resonance imaging, *J. Bone Mineral Res.*, **12**, 111–118.
- MANDELBROT, B. B. (1983) *The Fractal Geometry of Nature*, Freeman, New York, pp. 310–318.
- MANDELBROT, B. B. (1994) A fractal's lacunarity, and how it can be tuned and measured, in *Fractals in Biology and Medicine* (ed. T. F. Nonnenmacher, G. A. Losa and E. R. Weibel), Birkhäuser Verlag, Basel, pp. 8–21.
- PEISS, J., VERLANDE, M., AMELING, W. and GÜNTHER, R. W. (1996) Classification of lung tumors on chest radiographs by fractal texture analysis, *Invest. Radiol.*, **31**, 625–629.
- SAUPE, D. (1988) Algorithms for random fractals in *The Science of Fractal Images* (ed. H.-O. Peitgen and D. Saupe), Springer-Verlag, New York, pp. 71–136.
- SERRA, J. (1992) Dilation and filtering for numerical functions in *Image analysis and Mathematical Morphology Volume 2: Theoretical Advances* (ed. J. Serra), Academic Press, London, pp. 181–202.
- SERNETZ, M., WÜBBEKE, J. and WLCZEK, P. (1992) Three-dimensional image analysis and fractal characterization of kidney arterial vessels, *Physica A*, **191**, 13–16.
- STREICHER, J., WENINGER, W. J. and MÜLLER, G. B. (1997) External marker-based automatic congruencing: a new method of 3-dimensional reconstruction from serial sections, *Anat. Rec.*, **248**, 583–602.
- THIELE, D. L., KIMME-SMITH, C., JOHNSON, T. D., MCCOMBS, M. and BASSETT, L. W. (1996) Using tissue texture surrounding calcification clusters to predict benign vs malignant outcomes, *Med. Phys.*, **23**, 549–555.
- VEENLAND, J. F., GRASHUIS, J. L., VAN DER MEER, F., BECKERS, A. L. D. and GELSEMA, E. S. (1996) Estimation of fractal dimension in cardiographs, *Med. Phys.*, **23**, 585–594.
- VOSS, R. F. (1988) Fractals in nature: from characterization to simulation, in *The Science of Fractal Images* (ed. H.-O. Peitgen and D. Saupe), Springer-Verlag, New York, pp. 21–70.